Case Studies in Construction Materials 17 (2022) e01280

Contents lists available at ScienceDirect

Case Studies in Construction Materials

journal homepage: www.elsevier.com/locate/cscm

Case study

Study on strength formation and frost resistance of concrete modified by molybdenum tailings

Liu Fang, Fan Jiaqi *, Tang Ran, Zou Yuanrui

Key Laboratory of Concrete Structural Safety and Durability of Shaanxi Province, Xijing University, Xi'an, Shaanxi 710123, China

ARTICLE INFO

Keywords:
Strength formation
Frost resistance
Concrete
Freeze–thaw cycle
Molybdenum tailing material

ABSTRACT

Solid waste tailing materials from molybdenum mining in China occupy extensive land areas and threaten the health of nearby residents. To address the risk and the increasing shortage of natural construction materials, using those tailings as a construction material is a potential option for the construction industry. Modified concrete mixed with other tailings materials has been widely studied. The application of molybdenum tailings modified concrete to cold regions needs to fully consider its durability. Through the concrete cube compressive strength test and rapid freeze-thaw cycle test after different standard curing time, the strength formation process and frost resistance of molybdenum tailings modified concrete are explored. On this basis, the optimal content of Mo tailing material was determined. Results demonstrated that the compressive strength and frost resistance of Mo-tailing-modified concretes increased first and then decreased with the increase in Mo tailing content. The optimal modification effect was achieved when the Mo tailing content reached 20%. Under that circumstance, the porosity of Mo-tailing-modified concrete was at a minimum before and after the freeze–thaw cycles, thus increasing mechanical and antifrost properties significantly.

1. Introduction

With continuous global economic development, the demand for molybdenum (Mo) has gradually increased, accompanied by rapid growth in the yield and processing quantity of Mo ores [1]. Accompanying that, tailing emissions of low-grade Mo ore account for more than 95% of the low grade Mo during Mo exploitation, and they are processed by suspension technology. Storing these Mo tailings not only occupies vast land resources and increases the cost of construction and maintenance of tailings reservoirs, but also pollutes water and soil, inflicting considerable potential safety hazards on surrounding residential environments [2,3]. Therefore, promoting the extensive use of Mo tailings has attracted much attention [4]. With the research and development of new floating reagents, innovation of equipment, and updating of mineral processing technologies, the most valuable components in tailings can be recycled effectively. However, the tailing quantity is still very high, and the tailing storage problem has still not been solved effectively [5,6].

Using tailings as construction materials is attracting more and more attention as shortages of raw materials like aggregates become increasingly prominent [7–11]. Li Chun et al. [12] studied the preparation of baking-free bricks using Mo tailings and found that the mechanical properties of the bricks decreased with the increase in Mo tailing content. When the Mo tailing content was lower than 80%, it met the requirements of baking-free bricks (>MU10). Liu Zhenying [13] did an experimental study on the preparation of baking bricks made of Mo tailings. They shaped baking bricks following a certain mass ratio (7:3:0.3) of Mo tailings, clay, and sodium

* Corresponding author.
E-mail address: fanjiaqi1015@163.com (F. Jiaqi).

https://doi.org/10.1016/j.cscm.2022.e01280
Received 25 April 2022; Received in revised form 23 June 2022; Accepted 26 June 2022
Available online 27 June 2022

carbonate. Later, the shaped baking bricks were dried at 200 °C for 2 h, sintered at 1000 °C, then kept at that temperature for 3 h, thus producing sintered bricks. According to testing, the prepared bricks met China's index requirements for ordinary sintered bricks.

Producing ceramics with Mo tailings can not only achieve breakthroughs in traditional technologies that use clay as raw materials, but can also improve the performance of ceramics significantly. Li Bin [14] prepared ceramics using Mo tailings as raw materials and blast furnace slags of iron steel as additives. X-ray diffraction test results showed that the prepared ceramic was superior to similar products in terms of performance, and it could be used in building or corrosion industries, which could increase the use of Mo tailings to higher than 80%. Wang Xiulan et al. [15] prepared high-performance ceramics with compression moulding technology by using Mo tailings in Liaoning, China as major raw materials, with quartz and clay minerals as accessories. The prepared ceramics' density, flexural strength, and water absorption were 2.23 g/cm^3, 46.85 MPa, and 0.43% respectively. Zhang et al. [16] also prepared economical and durable ceramics by using Mo tailings as raw materials.

Because most buildings depend on concrete materials, preparing concretes with Mo tailing material can further increase the use of those materials in the construction industry [17,18]. Zhu Jianping et al. [19] prepared belite cement clinker by calcinating Mo tailings, limestone, and river sand (mass ratio = 23.30:73.00:3.4) at 1350 °C for 0.5 h. When gypsum (1.5% of total raw material mass) was added to the mixture, the strength of the clinker reached its peak. According to X-ray diffraction analysis, the volume fraction of the belite minerals was markedly higher than that of traditional portland cement. Cui Xiaowei et al. [20] implemented mechanical superfine grinding of Mo tailings, slags, cement clinker, and gypsum. Later, the powders were mixed at a mass ratio of 4:3:2:1, thus obtaining a binding material. By using stones as coarse aggregate and Mo tailings as fine aggregate, the concrete was prepared with a water-to-binder ratio of 0.26. The compressive strength of the prepared concrete reached 68.7 MPa. Liu Shichang [21] replaced river sand with tailings and prepared a high-strength concrete of composite binding material, pebble, and Mo tailings at a mass ratio (24.5:48.5:27) with a compressive strength of 70 MPa. Gao et al. [22–25] prepared concrete-filled steel tubular columns by replacing fine aggregate with Mo tailing material, which achieved a relatively good economic effect. Relevant research has proved the feasibility of Mo tailing materials in preparing modified concretes.

Existing studies on tailings concrete focus mainly on preparation and mechanical properties, but there are few studies on the durability of tailings concrete. However, the potential influences of tailing materials on the durability of concretes have been verified from multiple aspects [26–28]. Jamshid et al. [29] prepared concretes with copper tailings rather than cement and found that those solid waste tailings could be successfully used as a partial substitute for concrete cement. Moreover, a statistical analysis has shown that copper tailings have a significant influence on the durability of concrete. Mike et al. [30] used kimberlite tailings as concrete aggregates, which decreased the machinability of fresh concrete and increased water demands. If the mixing ratio was readjusted to overcome the defects of kimberlite tailings, the concrete performance could be improved.

The durability of concrete is closely related to its service environment, and it directly influences the engineering quality, safety, and service life of concrete structures. In cold regions, frost resistance is the ability of concrete to resist internal deterioration under freeze-thaw cycle conditions, which is the priority in durability indices, It is of great significance to improve the frost resistance of concrete in cold regions. Therefore, this study uses molybdenum tailings to prepare modified concrete, and explores how to improve the frost resistance of concrete after adding molybdenum tailings, studying the strength formation and frost resistance of Mo tailings modified concrete has a high theoretical value and engineering significance in guiding concrete engineering design in cold regions.

In this paper, molybdenum tailings was used to instead of fly ash to prepare modified concrete. The influences of Mo tailing content on concrete compressive strength and frost resistance were investigated through strength formation and freeze–thaw cycle tests. Finally, the optimal content of Mo tailing materials was determined in accordance with compressive strength and antifrost properties. The degradation of Mo-tailing-modified concretes during freeze–thaw cycles were determined through a computed tomography test.

2. Experimental methods

Experiments in this study were divided into compressive strength and freeze–thaw cycle tests. In those two tests, 150 mm × 150 mm × 150 mm concrete standard cubic specimens and 100 mm × 100 mm × 400 mm concrete prismoid specimens were prepared. The specimens were prepared in accordance with Chinese hydraulic concrete test codes (DL/T5150-2017). In the two tests, the molybdenum tailings content of the concrete specimens was the same, divided into 0%, 10%, 20%, 25%, and 30%, respectively.

2.1. Materials and equipment

The P•MH 42.5 moderate-heat Portland cement produced by the Sichuan Jiahua cement factory was used. Its physical and mechanical properties are shown in Table 1. The Mo tailing material and coal ash were collected from the Ruyang Yaochanggou tailings reservoir and the F-class I-level coal ash of the Henan Gongyi Yuanheng water purification material factory respectively. Fig. 1 depicts the particle size distribution of molybdenum tailings and fly ash, The density of molybdenum tailings material is 2.91 g/cm^3, and the

Table 1
Physical and mechanical properties of cements.

Specific Surface Area (m^2/kg)	Stability	Setting Time (min)		Flexural Strength (MPa)		Compressive Strength (MPa)	
		Initial Setting	Final Setting	3d	28d	3d	28d
338	Qualified	175	2442	5.2	10.5	31.8	42.6

density of fly ash is 2.42 g/cm^3. The primary chemical compositions of the cement, Mo tailing material, and fly ash are listed in Table 2. As fine aggregate, machine-made sand is used here with particle size less than 4.75 mm after mechanical crushing and screening (medium sand, fineness modulus of 2.77). The coarse sand was ordinary granite, with a grain size range of 5–40 mm, that of second-level grading. As a water reducer, HPEG-2400 polycarboxylate superplasticizer produced by Shandong Yousuo Chemical Engineering Technological Co., Ltd. was used, which was supplied in light yellow to white sheets. Its hydroxy value (mgKOH/g) was 22–27, pH value 5.0–5.7, and water $\leq$ 0.5%, which was dissolved in many organic solvents, including water. Water was collected from ordinary tap water in Xi'an City, China.

Test equipment included an MTS 2000 kN micro-electro-hydraulic servo universal testing machine, a TDR-28 concrete fast freeze–thaw test box, a DT-20 dynamic elastometer, and an MS-Voxe1450 industrial computerized tomography (ICT) scanner. The servo testing machine was used for the different standard curing times compressive strength tests of the cubic concrete specimens. The fast freeze–thaw tester simulated freeze–thaw cycle conditions effectively, and it was used to analyse the antifrost properties of the prismoid concrete species thoroughly in conjunction with the elastometer. The ICT scanner was used for computerized tomography of standard concrete specimens. It showed internal pore distribution and porosity changes in species clearly, and was also used for preliminary analysis of the freeze–thaw failures.

2.2. Test schemes

2.2.1. Mixing ratio and preparation process

The concrete studied in this paper will be considered to be applied to hydraulic concrete engineering in cold regions. Therefore, The mix proportion of concrete is calculated in accordance with the Chinese standard hydraulic concrete mix proportion design code (DL/T5330-2015). In this study, the doses of cement, fine aggregate, coarse aggregate, water reducer, and water were fixed. Five composite binding material systems of concretes were prepared by changing the mixing ratio of Mo tailing material and coal ash. The mixture without Mo tailing material (dose = 0%) was used as the control group, which was denoted as RC. The remaining four groups were test groups, in which the doses of Mo tailing material were 10%, 20%, 25% and 30%. Those four groups were denoted as $M_{10}C$, $M_{20}C$, $M_{25}C$, and $M_{30}C$ respectively. The detailed mixing ratios are shown in Table 3.

The concrete mixtures were prepared in accordance with the mixing ratios in Table 3. The stirred concrete mixtures were poured into 150 mm × 150 mm × 150 mm cubic moulds and 100 mm × 100 mm × 400 mm prismoid moulds. They were then compacted on a vibration table. Each group (RC, $M_{10}C$, $M_{20}C$, $M_{25}C$, and $M_{30}C$) comprised 15 standard cubic specimens and 3 prismoid species. Therefore, 75 standard cubic specimens and 15 prismoid species were prepared. After remaining static for 24 h, the specimens were demoulded using an air compressor. Subsequently, all specimens were cured in a standard incubator at 20 ± 2 °C and 95% relative humidity.

2.2.2. Compressive strength and frost resistance tests

The compressive strength test of concrete cubes was used to study the influences of Mo tailing content on the ultimate compressive strength of concrete for various durations. Three specimens were chosen from each group (RC, $M_{10}C$, $M_{20}C$, $M_{25}C$, and $M_{30}C$) at 1 d, 7 d, 14 d, 28 d, and 45 d for the test. The compressive strength test of concrete cubes covered 75 tests. The test schemes are summarised in Table 4. During the test, in order to ensure the accuracy of the cube compressive strength results, it is necessary to make the compressive area of the specimen in contact with the universal testing machine reach 100%. The loading rate of the universal testing machine was adjusted to 0.5 MPa/s, and uniform loading was applied. During the test, the specimens' stress–strain variation curves

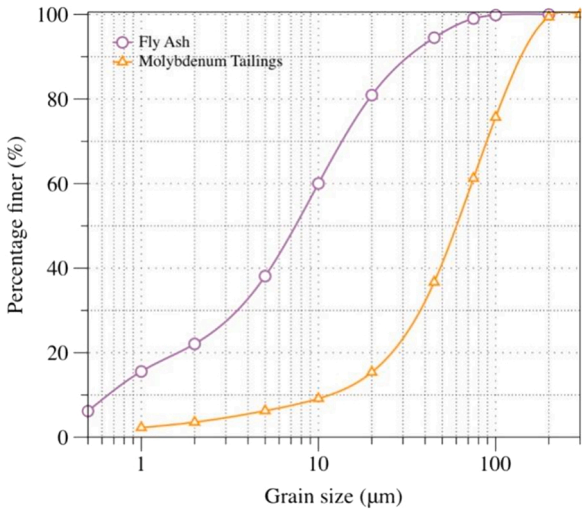

Fig. 1. Particle size of molybdenum tailings and fly ash.

Table 2
Major chemical compositions of cement, Mo tailing material, and fly ash (%).

Raw Material	SiO_2	Al_2O_3	CaO	Fe_2O_3	MgO	SO_3	Loss
Cement	21.0	3.95	61.0	5.04	4.22	1.98	1.47
Molybdenum Tailings	45.26	6.29	9.67	11.22	–	–	12.70
Fly Ash	53.36	29.09	2.27	3.87	0.81	–	2.86

Table 3
Mixing ratios of concretes (kg/m^3).

Group	Replacement amount of molybdenum tailings	Water	Cement	Fly Ash	Molybdenum Tailings	Fine Aggregate	Coarse Aggregate	Water Reducer
RC	0%	180	252	108	0	736	1104	2.7
$M_{10}C$	10%			82.8	25.2			
$M_{20}C$	20%			57.6	50.4			
$M_{25}C$	25%			45.0	63.0			
$M_{30}C$	30%			32.4	75.6			

Table 4
ANOVA of compressive strength.

Age (d)	RC (0%)	$M_{10}C$ (10%)	$M_{20}C$ (20%)	$M_{25}C$ (25%)	$M_{30}C$ (30%)	Error Range
	Compressive strength average (MPa)					
1	10.1 ± 0.51	10.8 ± 0.18	12.6 ± 0.12	11.5 ± 0.34	10.6 ± 0.49	< 3%
7	17.4 ± 0.38	18.4 ± 0.08	19.7 ± 0.28	18.8 ± 0.44	18.1 ± 0.10	
14	25.2 ± 0.08	25.9 ± 0.72	26.6 ± 0.06	26.0 ± 0.27	25.6 ± 0.34	
28	28.2 ± 0.11	30.2 ± 0.23	34.0 ± 0.48	31.9 ± 0.09	29.7 ± 0.51	
45	33.7 ± 0.21	35.9 ± 0.82	39.3 ± 0.91	37.0 ± 0.51	36.0 ± 0.33	

were recorded continuously, and the ultimate compressive strengths of the specimens were calculated.

The frost resistance test was used to study the influences of Mo tailing content on the frost resistance of concrete under freeze–thaw cycles. According to the requirements of concrete frost resistance test in the Chinese Standard Hydraulic Concrete Test Regulations (DL/T5150-2017), the mass loss rate and relative dynamic elastic modulus were analysed as the evaluation index of frost resistance, All concrete prismoid specimens of RC, $M_{10}C$, $M_{20}C$, $M_{25}C$, and $M_{30}C$ at 28 d were immersed in water for 4 d, then put into the fast freeze–thaw test box, as shown in Fig. 2. The lowest and highest temperatures in the fast freeze–thaw test box were set at -18 ± 2 ℃ and 5 ± 2 ℃ respectively. (one freeze-thaw cycle lasts 2.5–4.0 h, where temperature reduction process lasts 1.0–2.5 h, and the temperature rise lasts 1.0 h~2.0 h.) Specimens were taken out after 0, 50, 100, and 150 freeze–thaw cycles and weighed. Meanwhile, the dynamic elastic modulus was measured by the dynamic elastometer. The concrete specimens under different freeze-thaw cycles were scanned by ICT, as shown in Fig. 3.

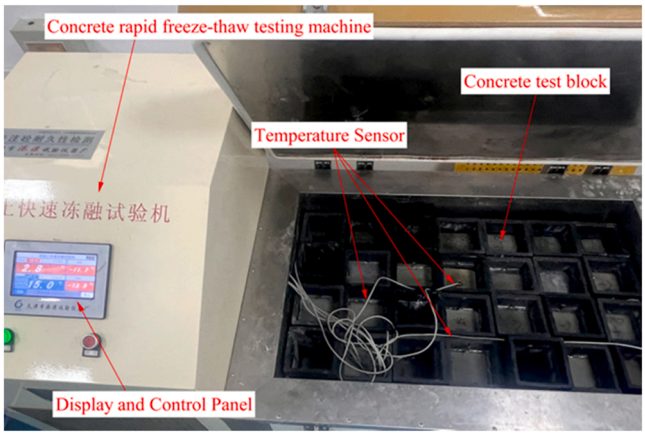

Fig. 2. Rapid freeze-thaw cycle test for concrete.

3. Test results and discussion

3.1. Different curing times compressive strength test

The one-way analysis of variance (ANOVA) of the compressive strengths of the cubic concrete specimens at various times is shown in Table 4. The error of the ultimate compressive strength was no higher than 3%. As the standard curing time increases, the compressive strengths of all specimens with different mixing ratios increased nonlinearly. The growth rate increased quickly in the first 14 d, then it decreased. Additionally, the concrete compressive strengths of the different groups diverged gradually with the increase in times. The concrete compressive strength of RC (0%) was at a low level at all times, indicating that mixing Mo tailings could increase concrete compressive strength effectively. The concrete compressive strength of $M_{20}C$ (20%) was markedly higher than that of the other four groups at all times. The $M_{20}C$ (20%) had the maximum compressive strength.

Fig. 4 shows that with the increase in Mo tailing content, the cube compressive strength of concrete increased first and then decreased. Under each standard curing time, the compressive strength of the specimens increased the most when the Mo tailing content was 20%. In the process of strength formation, the strength of modified concretes with various contents of Mo tailings increased greatly at 1 d, indicating that mixing Mo tailings could improve the early strength of concrete effectively. Subsequently, the rate of increase of the concrete strengths of all groups decreased gradually (decelerated hydration rate) until 28 d, when the strength began to increase greatly again. This showed that the hydration rates at 1 d and 14–28 d after adding Mo tailings were high, but the hydration rate at 28 d decreased.

The variation curves of the compressive strengths of concrete cubes with various Mo tailing contents at different standard curing times are shown in Fig. 5. Combined with Fig. 2, it is evident that the concrete compressive strength increased when the Mo tailing content was 0–10%, but the growth rate was low. The concrete compressive strength increased quickly when the Mo tailing content was 10–20%, and the growth rate increased. The concrete compressive strength began to decrease when the Mo tailing content was 20–25%, but it was still higher than that at 10%. The concrete compressive strength continued to decrease when the Mo tailing content was 25–30%, and it was close to that at 10%. The use of molybdenum tailings instead of fly ash as an admixture can fill the internal pores of the concrete to a large extent, making the concrete more dense and reducing the porosity [31]. In addition, the active components in molybdenum tailing materials, such as SiO_2, will react with $Ca(OH)_2$ to promote concrete hydration and generate a large amount of hydrated calcium silicate and ettringite, thereby improving concrete strength [32,33]. As the content of molybdenum tailings increases, the excess molybdenum tailings are not cemented together, which reduces the strength of the concrete [34].

Curves at different standard curing times all reflected the nonlinear relation between Mo tailing content and concrete compressive strength. The cube compressive strength of concrete reached the maximum when the Mo tailing content was approximately 20%. The shadow part of Fig. 5 shows that the concrete compressive strength increased significantly when the Mo tailing content was 19–21%.

The fitting curves and parameters between the ultimate compressive strengths and standard curing times are shown in Fig. 6 and Table 5. There was a logarithmic relation between age and ultimate compressive strength of the concrete cubic specimens. The influences of Mo tailing material on concrete strength were concentrated in the coefficient stage of the log function; that is, the Mo tailing material coefficient. The Mo tailing material coefficient was further fit with Mo tailing content. In that way, the function model of Mo-tailing-modified concrete compressive strength with different standard curing times and Mo tailing content could be gained (Fig. 7). A constructive model of Mo-tailing-modified concrete compressive strength during strength formation could be speculated:

$$N = (aM^2 + bM + c)\ln(D + e)$$

where N is the concrete compressive strength; M is the Mo tailing content; D is the curing age of concrete; and a, b, c, e are constant coefficients, which were − 0.0037, 0.1280, 0.4725, and 2.1867 respectively.

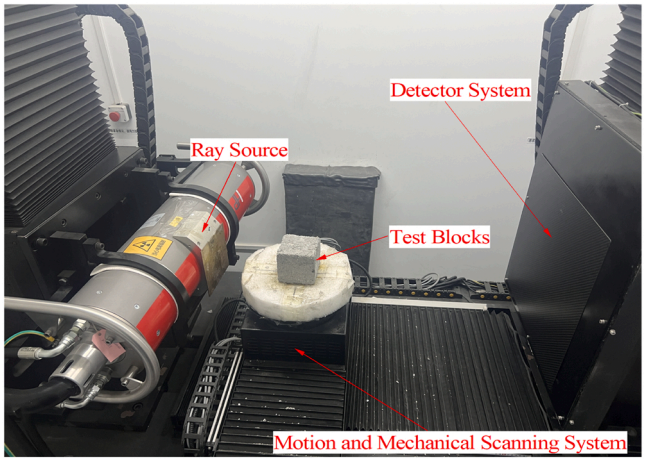

Fig. 3. ICT tomography test of concrete specimens after freeze-thaw cycles.

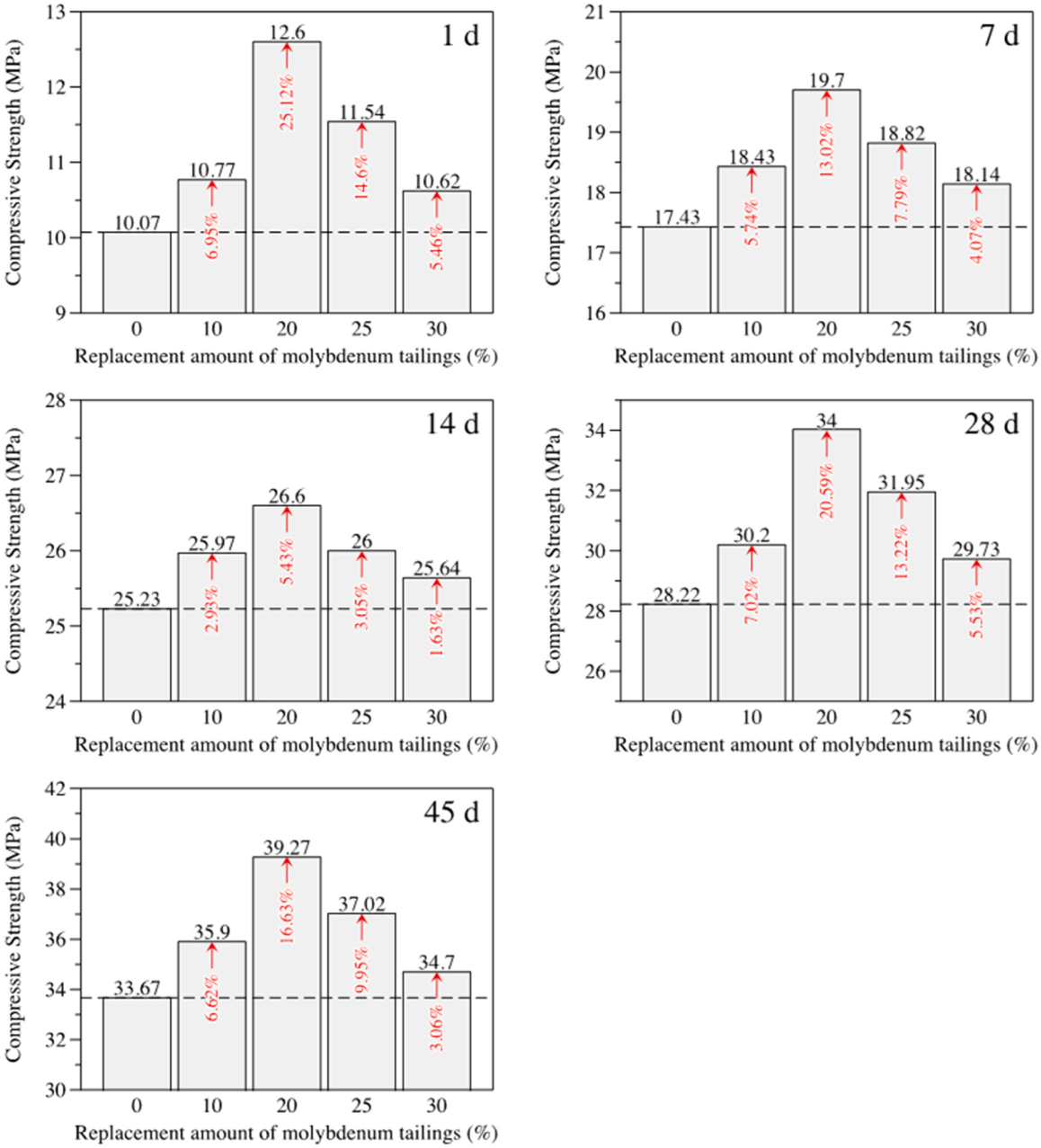

Fig. 4. Comparison of ultimate compressive strengths of specimens at various different curing times.

3.2. Freeze–thaw cycle test

The variation curves of the mass-loss rate and relative dynamic elastic modulus of the concrete cubic specimens with various Mo tailing contents under freeze–thaw cycles are shown in Figs. 8 and 9 respectively. Under freeze–thaw cycles, the mass-loss rate of different concrete cubic specimens increased gradually, whereas the relative dynamic elastic modulus decreased gradually. The mass-loss rate of RC (0%) increased the most, and its relative dynamic elastic modulus decreased the most. That showed that the frost resistance of concrete specimens without the Mo tailing material were poorer than those with the material. The test groups' mass-loss rates and relative dynamic elastic moduli decreased and increased to different extents. Compared with the other four groups, $M_{20}C$ (20%) had the lowest mass-loss rate throughout the freeze–thaw cycles, and the growth rate was also low. Moreover, the relative dynamic elastic modulus decreased slowest in the freeze–thaw cycles.

To a certain extent, molybdenum tailings may fill some of the pores inside the concrete, so that the internal pores of the concrete become lower, and the space for the freezing and expansion of water inside the pores becomes smaller. In addition, the molybdenum

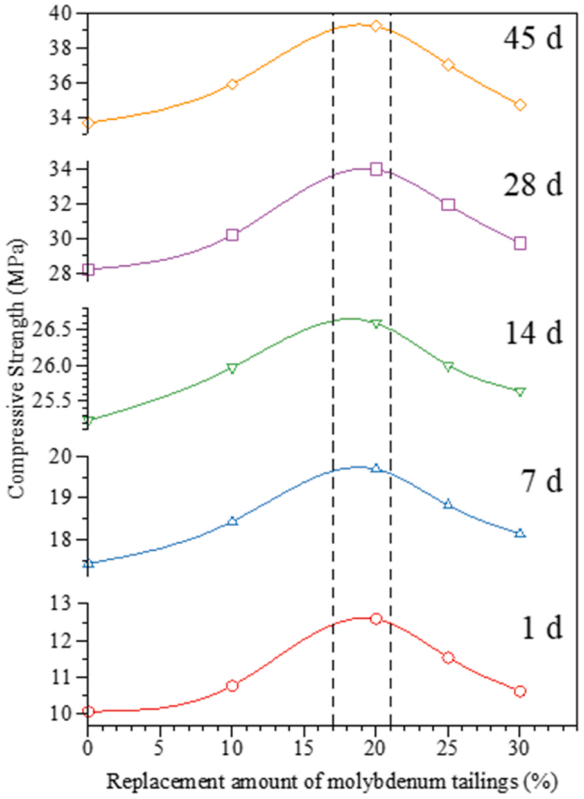

Fig. 5. Relation curves between Mo tailing content and ultimate compressive strength of concrete cubic specimens at various different curing times.

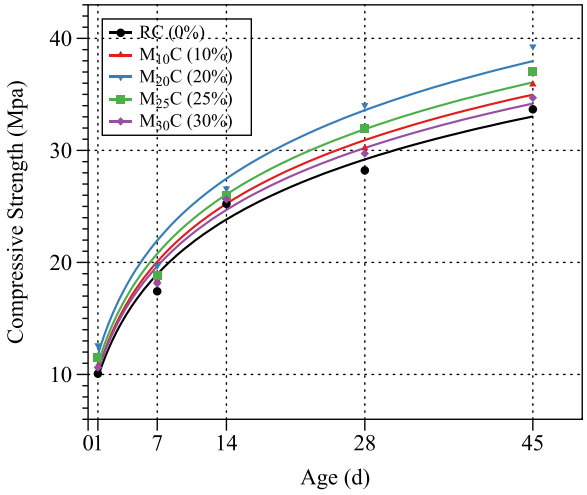

Fig. 6. Fitting curves between ultimate compressive strength of concrete cubic specimens and different curing times.

tailings material also contains some active ingredients such as SiO_2, which react with $Ca(OH)_2$ during the formation of concrete strength to promote hydration and greatly enhance the ability of concrete to resist expansion stress [32,33].

Figs. 10 and 11 compares the mass-loss rates of concrete prismoid specimens with various Mo tailing contents. With the increase in Mo tailing content, the mass-loss rate decreased first and then increased. When the Mo tailing content reached 20%, the mass loss in the freeze–thaw cycles was the lowest. At 150 freeze–thaw cycles, the mass-loss rate of RC (0%) was close to 5%, indicating that the specimens were going to fail. However, the mass-loss rate of $M_{20}C$ (20%) was 1.68%. With the increase in Mo tailing content, the variation evolution of the dynamic elastic modulus loss of specimens was similar to that of mass loss. Specifically, the dynamic elastic modulus loss rate decreased first and then increased when the Mo tailing content exceeded 20% (Fig. 9). At 150 freeze–thaw cycles, the

Table 5
Fitting parameters between ultimate compressive strengths of concrete cubic specimens and different curing times.

Group	Fit equation	R^2
RC (0%)	$y = 8.5736\ ln\ (x + 2.1217)$	0.98339
$M_{10}C$ (10%)	$y = 9.079\ ln\ (x + 2.1220)$	0.98775
$M_{20}C$ (20%)	$y = 9.8468\ ln\ (x + 2.3005)$	0.98156
$M_{25}C$ (25%)	$y = 9.3593\ ln\ (x + 2.2091)$	0.98758
$M_{30}C$ (30%)	$y = 8.8695\ ln\ (x + 2.1803)$	0.98937

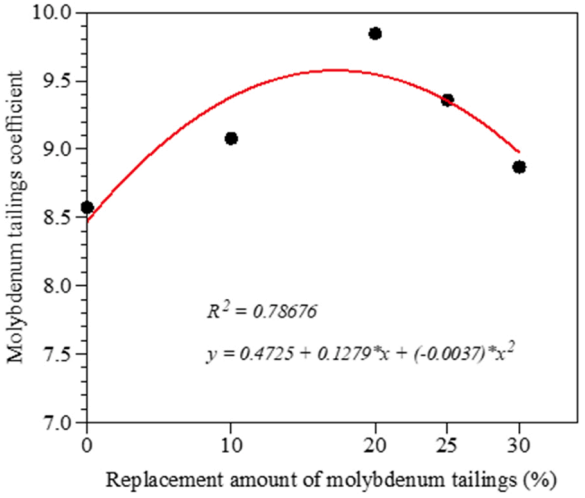

Fig. 7. Fitting curves of Mo tailing material coefficient.

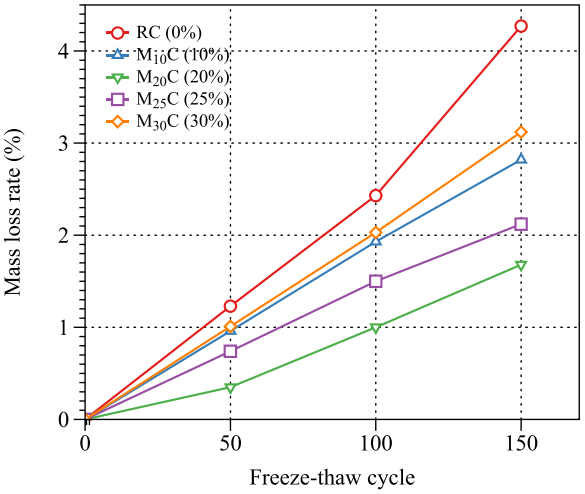

Fig. 8. Variation curves of mass-loss rate.

dynamic elastic modulus loss of RC (0%) reached 23.04%, but it was only 17.04% in the $M_{20}C$ (20%). Combining the mass loss and dynamic elastic modulus loss, $M_{20}C$ (20%) had the optimal indices of frost resistance.

3.3. Meso-analysis of freeze–thawing degradation

To further explore the mesostructure of Mo-tailing-modified concrete specimens under freeze–thaw cycles, the industrial CT scanner was applied to analyse the freeze–thaw degradation of Mo-tailing-modified concretes. In that way, the internal pore structure and evolution of the specimens were explored.

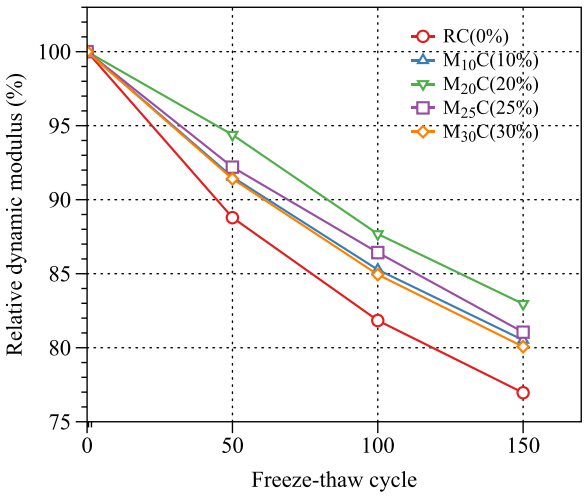

Fig. 9. Variation curves of relative dynamic elastic modulus.

3.3.1. *Pore changes of specimens with different Mo tailing contents*

The porosity of specimens with different Mo tailing contents and its variations are shown in Table 6. The variations refers to the porosity after 0 freeze-thaw cycles is used as the initial value here, and the porosity after 50 freeze-thaw cycles is used as the comparison value. The porosity of specimens and variations had trend of decreasing first and then increasing with increased Mo tailing content. The $M_{20}C$ (20%) had the lowest porosity and variation, which were consistent with the optimal Mo tailing content chosen in accordance with the compressive strength test and frost resistance test.

Both the mass-loss rate and the relative dynamic elastic modulus reflected the frost resistance of the concrete cubic specimens. There is a huge relationship between freeze-thaw damage and the porosity inside the concrete, the greater the porosity, the more serious the freeze-thaw damage [35,36]. For the analysis of ordinary concrete mesostructures subjected to freeze-thaw cycles, the lower porosity, the more compact internal structure of concrete and the better the frost resistance [37]. Combined with the porosity analysis of concrete specimens in Table 6, it was evident that adding appropriate Mo tailing material could increase the microstructural stability. This may be because with the increase of molybdenum tailings, firstly, the accumulation of particles is better and the porosity decreases [31]; In addition, the chemical composition of molybdenum tailings such as SiO_2 enhances the hydration, thereby improving the strength of concrete [32,33]. When the Mo tailing content was approximately 20%, the porosity of the concrete specimens was the lowest, and the resistance to the freezing expansion stress of pore water increased. Moreover, the corresponding mass-loss rate and relative elastic modulus of $M_{20}C$ (20%) were the best. This showed indirectly that concrete modified with a 20% Mo tailing content achieved good frost resistance.

3.3.2. *Porosity changes under different numbers of freeze–thaw cycles*

According to the evaluation based on mass-loss rate and relative dynamic elastic modulus, $M_{20}C$ (20%) had the best frost resistance. In this study, the porous structure of $M_{20}C$ in the freeze–thaw cycles was analysed.

The proportion of internal pore volume and the variation curves of total pore numbers in $M_{20}C$ under freeze–thaw cycles are shown in Fig. 12. The proportion of internal pore volume was divided into five ranges: < 0.01 mm^3, 0.01–0.1 mm^3, 0.1–1 mm^3, 1–10 mm^3, and ≥ 10 mm^3 [38–41]. With the increase in freeze–thaw cycles, concrete specimen surfaces began to peel off. Such surface peeling was severe after reaching a certain number of cycles. Because the volume of concrete specimens changed continuously, the porous structural evolution in the freeze–thaw cycles was analysed by the proportion of pores. Before freeze–thaw cycles (0 cycles), the proportions of pores in five size ranges of ($<$0.01 mm^3, 0.01–0.1 mm^3, 0.1–1 mm^3, 1–10 mm^3, $\geq$10 mm^3) decreased gradually. Before 50 freeze–thaw cycles, the proportions of pores of < 0.01 mm^3 and 0.01–0.1 mm^3 were relatively high. At 100–150 freeze–thaw cycles, the proportion of pores of < 0.01 mm^3 was the highest, followed by the proportion of pores of 1–10 mm^3. Generally speaking, pores of < 0.01 mm^3 in Mo-tailing-modified concretes predominated before 150 freeze–thaw cycles. With the increase in freeze–thaw cycles, the proportions of pores of < 0.01 mm^3, 0.01–0.1 mm^3, and 0.1–1 mm^3 in the $M_{20}C$ specimens generally had a descending trend, whereas the proportions of pores of 1–10 mm^3 and ≥ 10 mm^3 increased continuously. That showed that the internal structure of Mo-tailing-modified concretes degraded continuously in the freeze–thaw cycles, and small pores gradually evolved into large ones.

The porosity variations in various groups at 0 and 50 freeze–thaw cycles are shown in Fig. 13. The middle ICT scanner results of the specimens and 3D structural images of the pores are shown in Fig. 14. Combining Figs. 13 and 14 shows that the porosity of specimens increased gradually with the increase in freeze–thaw cycles. The blue part in the left represents the extracted pores, and different colours in the right show the 3D structure distribution of different volume size pores in concrete.(The pore volume $<$0.01 mm^3 is represented by red, 0.01–0.1 mm^3 is represented by yellow, 0.1–1 mm^3 is represented by blue, 1–10 mm^3 is represented by green, and $\geq$10 mm^3 is represented by white.) That was because the expansive force increased continuously as the pore water froze, thus increasing the pore sizes in the specimens. Under repeated freeze–thaw cycles, the number of internal pores in the specimens increased

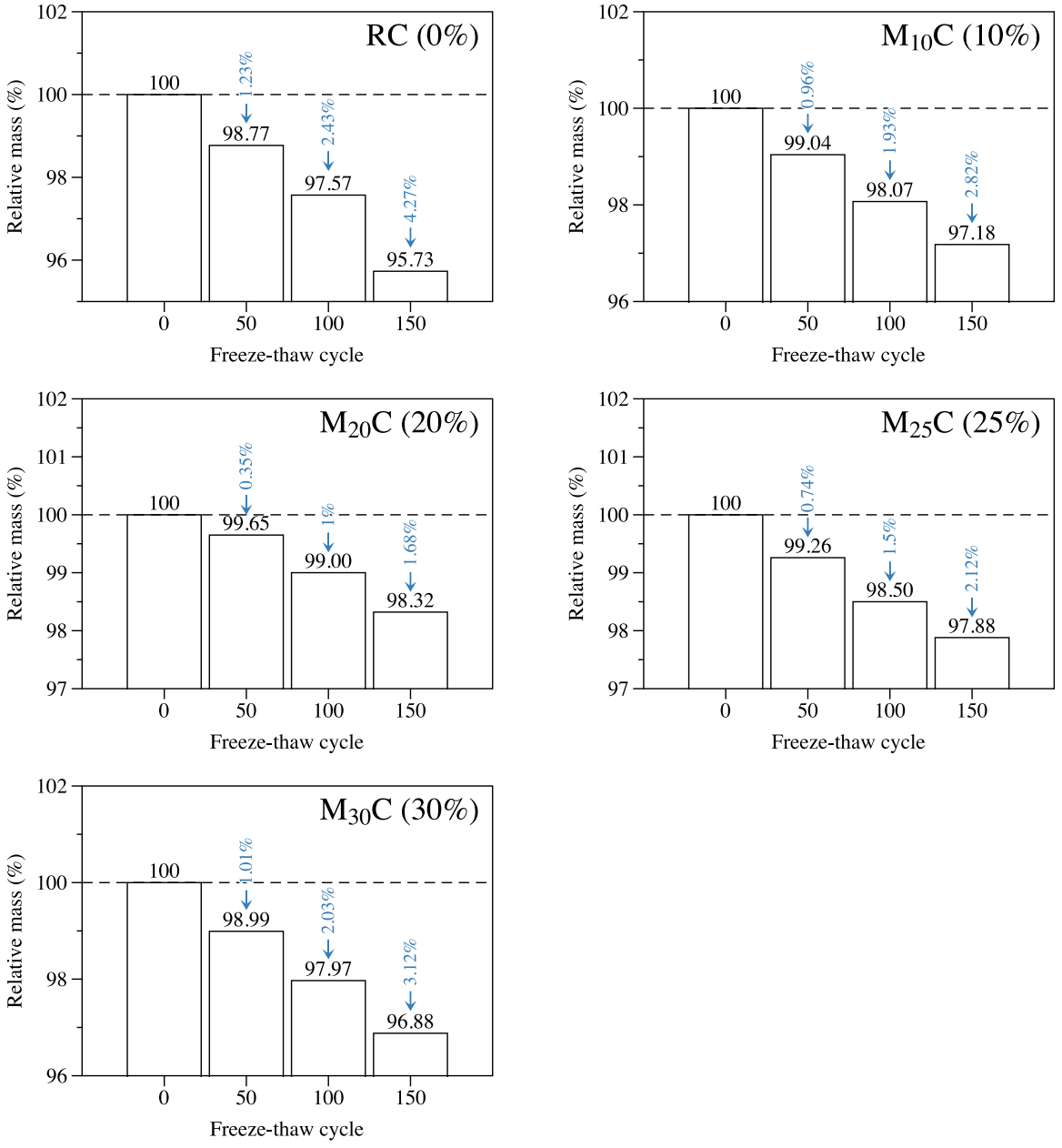

Fig. 10. Mass-loss rates of concrete prismoid specimens with various Mo tailing contents.

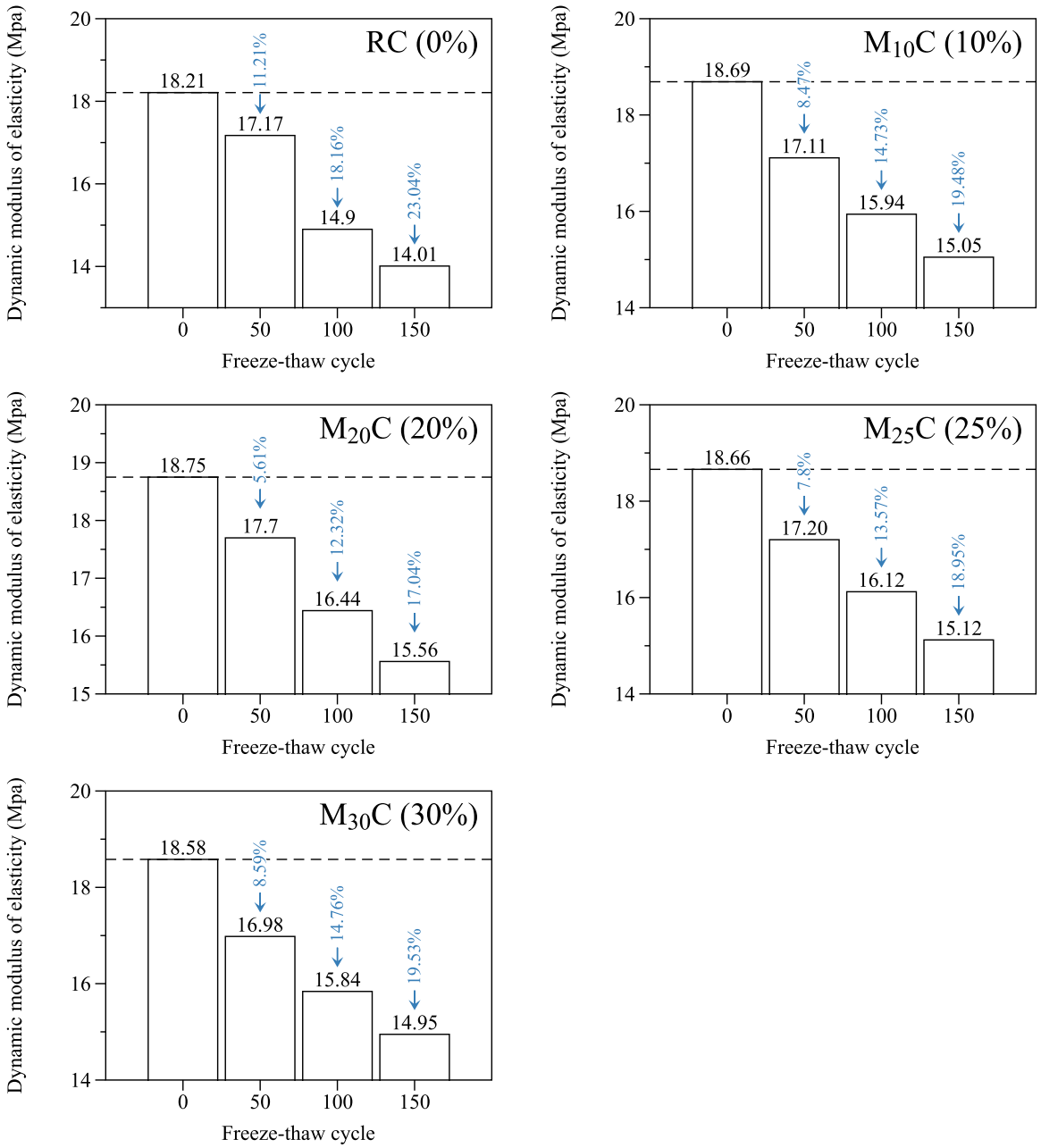

Fig. 11. Dynamic elastic modulus of concrete prismoid specimens with various Mo tailing contents.

Table 6
Porosity and variations.

Times	RC (0%)		$M_{10}C$ (10%)		$M_{20}C$ (20%)		$M_{25}C$ (25%)		$M_{30}C$ (30%)	
	Porosity	Variations	Porosity	Variations	Porosity	Variations	Porosity	Variations	Porosity	Variations
0	0.374	98.6%	0.233	74.9%	0.080	30.2%	0.131	41.8%	0.281	69.5%
50	0.743		0.408		0.104		0.186		0.476	

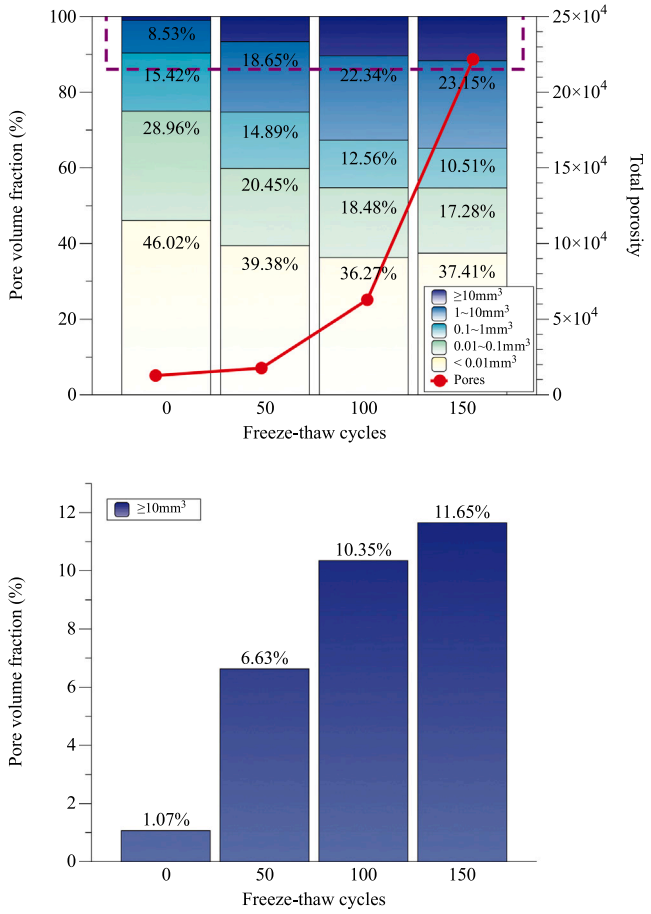

Fig. 12. Variations in internal pore volumes of $M_{20}C$ specimens under various numbers of freeze–thaw cycles.

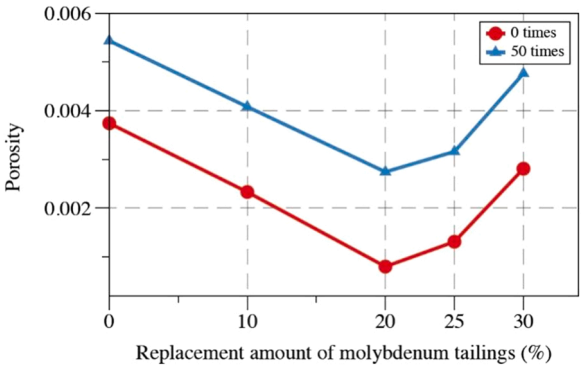

Fig. 13. Variations in internal pore volumes of different Mo tailing contents specimens under at 0 and 50 freeze–thaw cycles.

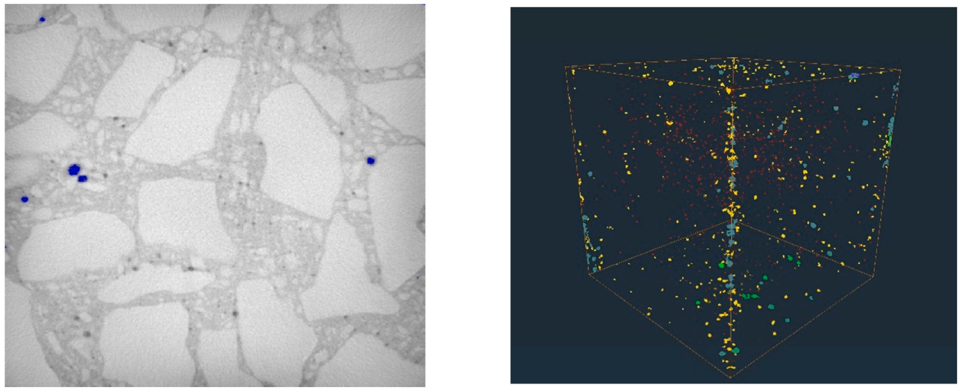

a. 0 cycles

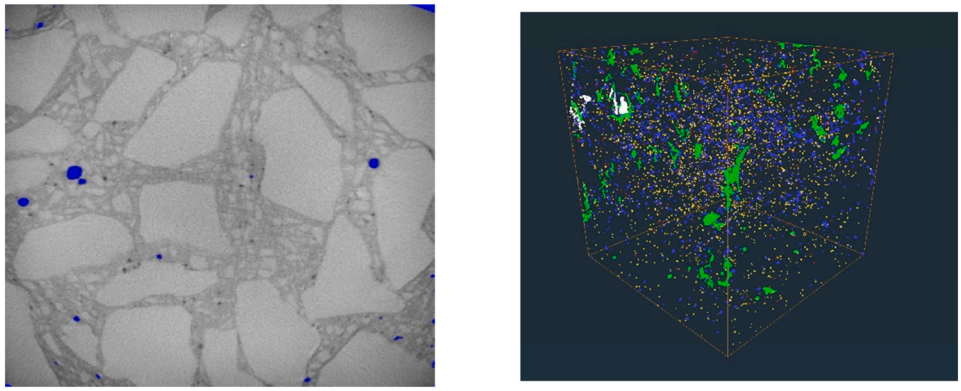

b. 50 cycles

Fig. 14. Middle ICT scanner results of $M_{20}C$ and 3D structural images of pores.

continuously. Specifically, the number of large pores increased continuously, which was the primary cause of the specimens' failure. Using Mo tailing material as a binding material strengthened the internal bonding of concrete and significantly increased water migration. As a result, pores were filled in, and the pore water content decreased. The expansion stress resistance of the specimens under freeze–thaw cycles increased significantly.

4. Conclusions

In this study, concrete compressive strength and freeze–thaw cycle tests were done to study the age compressive strength and antifrost properties of concretes with different Mo tailing contents. A micro-analysis of freeze–thaw degradation of Mo-tailing-modified concretes was done by using ICT scans to determine the internal degradation and evolutionary of concrete porous structures under freeze–thaw cycles. Some major conclusions could be drawn:

1. According to different standard curing times compressive test results, Mo tailing material can increase concrete compressive strength. The concrete compressive strengths at all times demonstrate that the best compressive strength can be achieved when the Mo tailing content is approximately 20%. With collaborative considerations of different standard curing times compressive strength and Mo tailing content, the relation of the different standard curing times of Mo-tailing-modified concretes to their compressive strength were summarised, which provides a basis for practical applications of Mo tailing material.

2. The freeze–thaw cycle test results show that Mo tailing material can obviously improve the frost resistance of concrete. When Mo tailings were added, the mass-loss rate and relative dynamic elastic modulus loss rate of concrete both decreased to some extent under different numbers of freeze–thaw cycles. Moreover, the mass-loss rate was no higher than 5%, and the dynamic elastic modulus did not decrease to lower than 60%. According to the antifrost properties of concrete cubic specimens under different freeze–thaw cycles, the best antifrost properties were achieved when the Mo tailing content was approximately 20%.

3. Based on a CT analysis, the pore volume fraction of concrete specimens with different Mo tailing contents had showed a trend of decreasing at first and then increasing, which reached the minimum when the Mo tailing content was 20%. For concrete specimens with a 20% Mo tailing content, porosity was positively related to the number of freeze–thaw cycles. With the increase in freeze–thaw

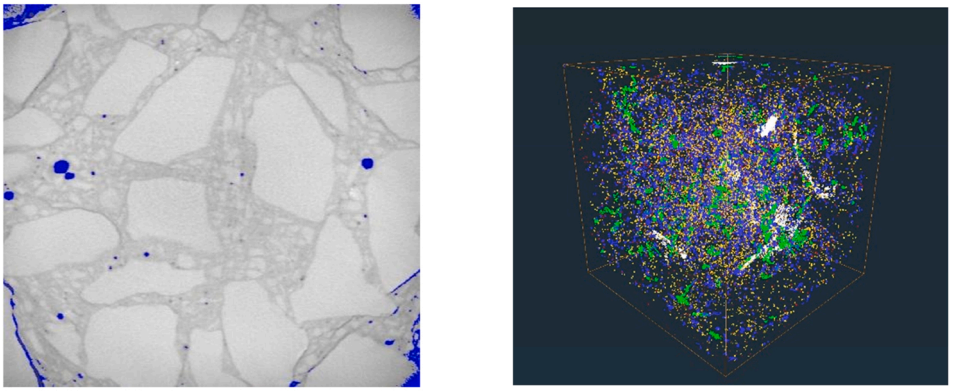

d. 100 cycles

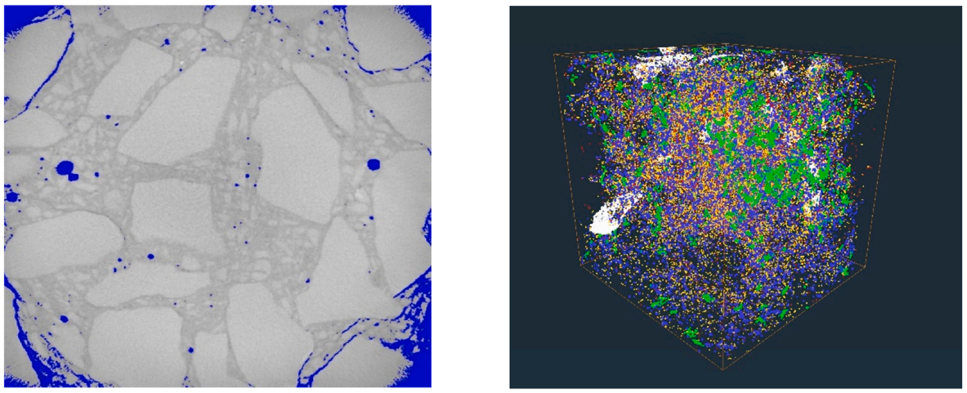

e. 150 cycles

Fig. 14. (*continued*).

cycles, the proportion of internal pores changed accordingly, and small pores developed into large pores, thus gradually increasing the number of cracks and degrading the performance of the concrete.

4. According to the analysis of the above, when molybdenum tailings are used to replace fly ash to prepare modified concrete, the active components in molybdenum tailings, such as SiO_2, will react with $Ca(OH)_2$ to promote the hydration of concrete, thus improving the strength of concrete. At the same time, the addition of molybdenum tailings fills the pores in the concrete, reducing the porosity. Therefore, the internal structure is more compact, which improves the frost resistance of the concrete and delays the deterioration caused by the freeze-thaw cycle.

Declaration of Competing Interest

The authors declare that they have no known competing financial interests or personal relationships that could have appeared to influence the work reported in this paper.

Data availability

Data will be made available on request.

Acknowledgements

This work is supported by the National Natural Science Foundation of China [51902270]; the Special Fund for the Launch of Scientific Research in Xijing University [XJ21T01]; the Youth Innovation Team of Shaanxi Universities.

References

[1] F. Huang, Y.C. Chen, D.H. Wang, Z.X. Yuan, Z.H. Chen, A discussion on the major molybdenum ore concentration areas in China and their resource potential, Geol. China 38 (2011) 1111–1134, https://doi.org/10.1007/s12583-011-0163-z.

[2] Z. Han, D. Wan, H. Tian, W. He, Z. Wang, Q. Liu, Pollution assessment of heavy metals in soilsand plants around a molybdenum minein central China, Pol. J. Environ. Stud. 28 (2018) 123–133, https://doi.org/10.15244/pjoes/83693.
[3] Z. Peng, X. Lin, Y. Zhang, Z. Hu, X. Yang, C. Chen, H. Chen, Y. Li, J. Wang, Removal of cadmium from wastewater by magnetic zeolite synthesized from natural, low-grade molybdenum, Sci. Total Environ. 772 (2021), 145355, https://doi.org/10.1016/j.scitotenv.2021.145355.
[4] S.I. Evdokimov, M.P. Maslakov, V.S. Evdokimov, Construction materials based on wastes from mining and metallurgical industries, Procedia Eng. 150 (2016) 1574–1581, https://doi.org/10.1016/j.proeng.2016.07.120.
[5] C. Yu, Study on Migration and Transformation of Heavy Metals in Alkaline Mo Tailings and Affected Water (Ph.D.), Dalian University of Technology, 2010.
[6] L. Ou, C. Qi, Depressing of polysaccharides in floating separation of talc from molybdenite of non-polar surface minerals, Metal Mine 000 (2015) 85–89.
[7] M.Y. Jung, Y.W. Choi, J.G. Jeong, Recycling of tailings from Korea Molybdenum Corporation as admixture for high-fluidity concrete, Environ. Geochem. Health 33 (2011) 113–119, https://doi.org/10.1007/s10653-010-9355-1.
[8] Y. Tan, Y. Zhu, H. Xiao, Evaluation of the hydraulic, physical, and mechanical properties of pervious concrete using iron tailings as coarse aggregates, Appl. Sci. 10 (2020) 2691, https://doi.org/10.3390/app10082691.
[9] J. Xue, X. Wang, Z. Wang, S. Xu, H. Liu, Investigations on influencing factors of resistivity measurement for graphite tailings concrete, Cem. Concr. Compos. 123 (2021), 104206, https://doi.org/10.1016/j.cemconcomp.2021.104206.
[10] F. Han, S. Song, J. Liu, S. Huang, Properties of steam-cured precast concrete containing iron tailing powder, Powder Technol. 345 (2019) 292–299, https://doi.org/10.1016/j.powtec.2019.01.007.
[11] The influence of tailings and cement type on durability properties of self-compacting concrete, Teh. Vjesn. 24 (2017), https://doi.org/10.17559/TV-20160304113800.
[12] C. Li, E. Wang, L. Cui, X. Cui, Y. Di, C. Zhou, Preparation of unfired brick by molybdenum tailings of Shangluo, New Build. Mater. 43 (2016) 3, https://doi.org/10.3969/j.issn.1001-702X.2016.07.023.
[13] Z. Liu, Experimental research on production of sintered bricks from molybdenum mine tailings, China Nonmet. Min. Ind. Guide (2011) 2, https://doi.org/10.3969/j.issn.1007-9386.2011.04.012.
[14] B. Li, Z. Sui, The study on molybdic tailing glass, China Ceram. Ind. 8 (2001) 15–16.
[15] X. Wang, D. Tian, H. Shi, G. Wang, Preparation and performances of building ceramic by molybdenum tailings, J. Synth. Cryst. 46 (2017) 4.
[16] J.R. Zhang, R. Wang, Preparation of glass-ceramics using molybdenum tailings, AMR 284–286 (2011) 1431–1434, https://doi.org/10.4028/www.scientific.net/AMR.284-286.1431.
[17] S. Siddique, J.G. Jang, Assessment of molybdenum mine tailings as filler in cement mortar, J. Build. Eng. 31 (2020), 101322, https://doi.org/10.1016/j.jobe.2020.101322.
[18] Z. Bai, K. Li, X. Ma, Z. Yang, X. Ma, Preparation and characterization of molybdenum tailings-based water storage material, Mater. Chem. Phys. 236 (2019), 121791, https://doi.org/10.1016/j.matchemphys.2019.121791.
[19] J. Zhu, H. Hou, H. Yin, B. Tan, K. Ren, X. Guan, Early performances of belite cement clinker from molybdenum tailings, Bull. Chin. Ceram. Soc. 34 (2015) 5, https://doi.org/10.16552/j.cnki.issn1001-1625.2015.07.020.
[20] X. Cui, Y. DI, H. Pang, N. Nan, X. Liu, C. Zhou, Research on preparation of high performance concrete with molybdenum tailings, Metal Mine (2017) 4.
[21] S. Liu, Study on preparation of high strength concrete by ultrafine particle molybdenum tailings, Hebei University of Engineering, 2017 (In Chinese).
[22] S. Gao, X. Cui, S. Kang, Y. Ding, Sustainable applications for utilizing molybdenum tailings in concrete, J. Clean. Prod. 266 (2020), 122020, https://doi.org/10.1016/j.jclepro.2020.122020.
[23] S. Gao, X. Cui, S. Kang, Y. Ding, Sustainable applications for utilizing molybdenum tailings in concrete, J. Clean. Prod. 266 (2020), 122020, https://doi.org/10.1016/j.jclepro.2020.122020.
[24] S. Gao, X. Cui, S. Zhang, Utilization of molybdenum tailings in concrete manufacturing: a review, Appl. Sci. 10 (2019) 138, https://doi.org/10.3390/app10010138.
[25] S. Gao, J. Qu, S. Zhang, L. Guo, Z. Huang, A comparative study on mechanical and environmental performance of concrete-filled steel tubes using molybdenum tailing aggregate, J. Constr. Steel Res. 189 (2022), 107100, https://doi.org/10.1016/j.jcsr.2021.107100.
[26] F.T. Al Rikabi, S.M. Sargand, I. Khoury, H.H. Hussein, Material properties of synthetic fiber–reinforced concrete under freeze-thaw conditions, J. Mater. Civ. Eng. 30 (2018) 04018090, https://doi.org/10.1061/(ASCE)MT.1943-5533.0002297.
[27] X.X. Feng, X.L. Xi, J.W. Cai, H.J. Chai, Y.Z. Song, Investigation of drying shrinkage of concrete prepared with iron mine tailings, KEM 477 (2011) 37–41, https://doi.org/10.4028/www.scientific.net/KEM.477.37.
[28] H. Yang, Z. He, Y. Shao, L. Li, Improving freeze-thaw resistance and strength gain of roller compacted fly ash concretes with modified absorbent polymer, J. Mater. Civ. Eng. 30 (2018) 04018010, https://doi.org/10.1061/(ASCE)MT.1943-5533.0002159.
[29] J. Esmaeili, H. Aslani, Use of copper mine tailing in concrete: strength characteristics and durability performance, J. Mater. Cycles Waste Manag. 21 (2019) 729–741, https://doi.org/10.1007/s10163-019-00831-7.
[30] M. Otieno, E. Ndoro, Utilization of kimberlite tailings as aggregates in concrete - strength and selected durability properties, MRS Adv. 5 (2020) 1259–1266, https://doi.org/10.1557/adv.2020.153.
[31] Z. Quan, X. Feng, Y. Chen, Study on the preparation of reactive powder concrete with molybdenum tailings, New Build. Mater. 49 (2022) 46–49.
[32] L. Xiaoying, L. Jun, L. Zhongyuan, H. Li, C. Jiakun, Preparation and properties of reactive powder concrete by using titanium slag aggregates, Constr. Build. Mater. 234 (2020), 117342, https://doi.org/10.1016/j.conbuildmat.2019.117342.
[33] Z. Luo, Z. Liu, Z. Si, X. Chen, S. Kang, Study of tail molybdenum ore mixed sand distribution optimization and the performance on the cement mortars, Concrete 107–109 (2018) 114.
[34] C. Wang, P. Ye, K. Zhang, G. Han, Z. Huo, G. Zhao, Z. Ren, Study on preparation and hydration mechanism of composite cementitious materials using molybdenum tailings, Metal Mine (2020) 41–47, https://doi.org/10.19614/j.cnki.jsks.202009005.
[35] H. Xue, X. Shen, C. Zou, Q. Liu, Y. Zou, Freze-thaw pore evolution of aeolian sand concrete based on nuclear magnetic resonance, J. Build. Mater. 22 (2019) 199–205, https://doi.org/0.3969/j.issn.1007-9629.2019.02.006. (In Chinese).
[36] R.E. S, P. Hatanaka, S. Palamy, Kurita, Experimental study on the porosity evaluation of pervious concrete by using ultrasonic wave testing on surfaces, Constr. Build. Mater. 300 (2021), 123959, https://doi.org/10.1016/j.conbuildmat.2021.123959.
[37] Z. Ding, N. Quy, T. Noguchi, J. Kim, Y. Hama, A study on the change in frost resistance and pore structure of concrete containing blast furnace slag under the carbonation conditions, Constr. Build. Mater. 331 (2022), 127295, https://doi.org/10.1016/j.conbuildmat.2022.127295.
[38] J. Liu, J. Xie, Y. Liu, P. Shi, Experimental study on concrete damage location by Computerized tomography and Acoustic Emission technology, Frat. Ed Integrità Strutt. 12 (2018) 352–360, https://doi.org/10.3221/IGF-ESIS.46.32.
[39] V. Cnudde, A. Cwirzen, B. Masschaele, P.J.S. Jacobs, Porosity and microstructure characterization of building stones and concretes, Eng. Geol. 103 (2009) 76–83, https://doi.org/10.1016/j.enggeo.2008.06.014.
[40] J.-Y. Fang, N. Li, F. Qu, Z.-S. Dou, S.-T. Li, Quantitative analysis of concrete on the basis of fuzzy set and computerised tomography number, Therm. Sci. 24 (2020) 3907–3913, https://doi.org/10.2298/TSCI2006907F.
[41] W. Tian, N. Han, Pore characteristics (>0.1 mm) of non-air entrained concrete destroyed by freeze-thaw cycles based on CT scanning and 3D printing, Cold Reg. Sci. Technol. 151 (2018) 314–322, https://doi.org/10.1016/j.coldregions.2018.03.027.